A New Approach to Inkjet Printing of High Viscosity Inks for 3D Applications

Stefan Güttler[1], Antonia Götz[1,2], Jan Christoph Janhsen[2], Anna Kolosova[1,2]

Abstract

Keywords: high viscosity inkjet, additive manufacturing, 3D printing, high frequency rheology, inkjet, manufacturing

Abstract

By combining recent advancements in high viscosity piezo inkjet and measurement technique for high frequency rheology, we investigate a route to multi-material printing of highly viscous UV polymers that were developed for vat photo polymerization. The targeted application is additive manufacturing of dental prosthesis where a single-material process (vat photo polymerization) shall be replaced by a multi-material process (inkjet printing) without compromising the material properties of the prosthesis. We study the printability of UV-polymers from two manufacturers with the recently introduced printhead from Quantica (a prototype). At temperatures of 60°C-70°C the viscosity and Ohnesorge number lie in a printable range. The integrity of the UV-polymers at elevated temperatures is tested. The (linear) visco-elasticity is studied by vibrational rheology in a frequency range up to 10kHz and a viscoelastic model (Maxwell-Wiechert model) of the materials is fitted to the data.

1. Introduction: Limitations of additive manufacturing and the role of piezo inkjet

Many additive manufacturing (AM) techniques have found their way into manufacturing of customized products in an industrial scale overcoming their former limitation to prototyping. An overview over additive manufacturing can be found in [ISO/ASTM 52900, 2021]. Additive manufacturing processes can be categorized according to their functional principles. In powder-based processes layers of spread powder (metal or thermoplastic polymer) are either selectively sintered or molten (powder bed fusion – PBF) or fixed by a binder that is printed into

[1]Fraunhofer Institute for Manufacturing Engineering and Automation; [2]Stuttgart Media University

the powder bed (binder jetting – BJ). The glued powder is subsequently sintered or infiltrated with a resin. A widespread process is melting of a thermoplastic filament that solidifies layer by layer into a 3D shape (material extrusion – MEX). Other AM techniques depend on curing of UV-polymers. A UV polymer in a vat is selectively cured by a laser, digital light projector, or LC screen, layer by layer (vat photo polymerization) or UV inks are layer by layer printed by piezo inkjet and cured. (Material jetting – MJ). The properties of the various additive manufacturing techniques widely differ depending on the material and manufacturing method.

What all additive manufacturing technologies have in common is the limitation of the materials that can be processed. All methods but material jetting and material extrusion are limited to a single building material. MEX can extrude materials strand by strand whereas material jetting with piezo inkjet allows to deposit materials drop by drop (voxel by voxel). This enables tailoring the optical or mechanical properties of a 3D structure by combining a set of process materials (like color synthesis from process colors CMY).

An important application of AM is manufacturing of medical prosthesis. Building of customized structures of any desired shape is a clear strength of AM as far as the strict requirements on the material properties can be met. On today dental prosthesis as crowns, dentures, splints, and surgical templates are manufactured by vat photo polymerization. Progress in the development of UV polymers allowed to extend the usage of additive manufactured dental prosthesis from provisory use over temporal to permanent use. Main disadvantage of vat photo polymerization is the restriction to a single building material. For manufacturing of (permanent) dentures or crowns shades of color and transparencies need be precisely reproduced what requires expensive manual retouching.

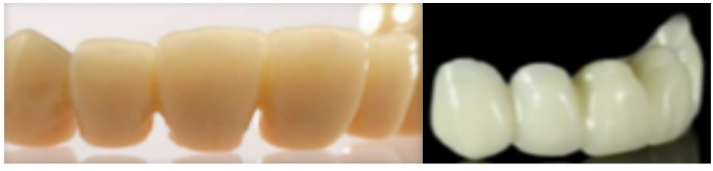

Figure 1: *Additive manufactured dental prosthesis (by vat photo polymerization)*

Inkjet printing of UV polymers allows printing of several materials, e.g. colors. But a major limitation of piezo inkjet is the viscosity of printable inks. Polymers designed for vat photo polymerization have a viscosity higher than 1000mPas at room temperature. The viscosity of inks for standard piezo printheads is limited to at most 25mPs at operating temperature. The operating temperature depends on the printhead and can go up to 125°-130°C for hot-melt printheads [Specifications of hot melt printheads]. The viscosity of polymers strongly decreases with rising temperature but many functional materials do not withstand such elevated temperatures. Moreover, the diameter of particles (ceramic fillers, pigments) in inkjet inks need be small (d_{90} <1-3µm, depending on nozzle size), and the volume

fraction of solids cannot be too high. Inkjet inks must be chemically stable (free of sedimentation). In printheads with ink circulation a slow sedimentation of solids is tolerable if particles can be redispersed.

After piezo inkjet found its way into industrial applications as of around 2000 many attempts were made to extend the viscosity range of inks. After the physics of piezo inkjet was understood it became clear that the functional principle of piezo inkjet limits the viscosity of printable inks. For medium viscous inks (~15-20mPas) the pressure drop caused by viscous dissipation in the nozzle consumes most of the pressure generated at the nozzle. The maximal pressure in a piezo printhead is limited because the positive pressure wave that accelerates the ink in the nozzle is accompanied by negative pressure waves due to reflections of the sound wave in the printhead cavity. A too strong positive pressure wave cannot avoid strong negative pressure waves that draw air through the nozzle into the pumping chamber what defeats the pumping mechanism. A comprehensive treatment of the functional principle of piezo inkjet printheads is found e.g. in the pioneering works [Wijshoff, 2008; Wijshoff, 2010].

Beside the technical limits of piezo printheads also a physical border for the detachment of drops from a fluid surface (capillary, nozzle) through a Plateau-Rayleigh instability exist. This is the mechanism of drop formation in all inkjet printheads except electro-hydrodynamic inkjet. Two time scales control the breakup of a cylinder of a Newtonian fluid:

$$t_R = \sqrt{\frac{\rho d^3}{\sigma}} \quad \text{and} \quad t_\eta = \frac{\eta d^3}{\sigma}$$

where η, ρ, σ are the viscosity, density, and surface tension of the fluid. d is the diameter of the fluid cylinder or nozzle. See e.g. [Pekker, 2018] for a discussion of the breakup of a cylinder of viscous liquid. With increasing viscosity, the detachment of drops through a Plateau-Rayleigh instability becomes slower what eventually prevents any inkjet process that depends on this mechanism. For Newtonian fluids, the detach-ment of drops from a fluid surface and the printability of fluids by piezo inkjet is characterized by the Ohnesorge number:

$$\text{Oh} = \frac{t_\eta}{t_R} = \frac{\eta}{\sqrt{\rho \bullet d \bullet \sigma}}$$

According to [Derby, 2010] (Newtonian) fluids are printable by piezo inkjet in the range ~0,1 < Oh < ~1 and:

$$\text{We} = \frac{p \bullet d \bullet v^2}{\sigma}$$

(Weber number) where v is the drop speed (*Fig. 2*). Many highly viscous fluids are non-Newtonian and their printability cannot be fully characterized by the Ohnesorge number.

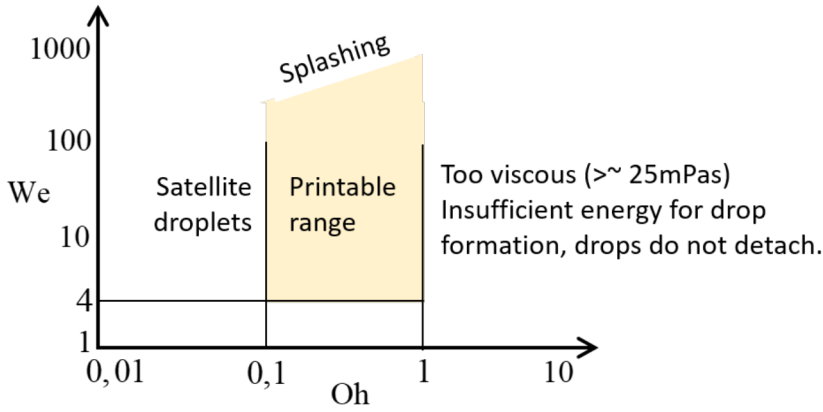

Figure 2: *Range of printable fluids according to [Derby, 2010]*

Attempts have been made to develop digital printing techniques that overcome the technical limitations of piezo inkjet. Laser Transfer Printing (LTP) is a non-contact printing technique based on the Laser Induced Forward Transfer process (LIFT) introduced in 1986 [Serra, 2019]. LTP is able to print inks with much higher viscosity, larger particle diameter and higher volume fraction of solids than inkjet can. A disadvantage of LTP is the drop generation mechanism that depends on formation of a vapor bubble. This requires inks that can form vapor bubbles or a sacrificial layer for bubble formation placed beneath the ink film. LFT print engines are large and much more expensive than piezo inkjet engines. This limits the benefit of LTP for multi-material applications.

Most recently Scrona (CH) introduced a novel electro-hydrodynamic (EHD) printhead [Galliker, 2024]. Drop formation in EHD printheads does not depend on a Plateau-Rayleigh instability. As a consequence, compared to piezo inkjet the viscosity range is much larger. Drop volumes can be less than 1fl (10^{-3}pl, ~1000 times smaller than drops in piezo inkjet can be). Disadvantage is the complicated design of EHD printheads what puts up challenges to manufacture them. To date, EHD printing is a laboratory technique with print engines/printheads having a single or few nozzles.

Well-known micro dispensing devices can extrude a filament of viscous fluid and cut it by a valve. Micro dis-pensers have a single or few nozzles which are large and expensive. The dispensing frequency is low.

Recently Xaar (GB) and Quantica (Germany) developed piezo printheads with an enlarged viscosity range that allow printing of fluids with viscosity up to 60-100mPas, possibly more [Jackson, 2019; Borrell, 2022]. The Quantica printhead is not an acoustic printhead, its functional design differs from other piezo print-heads. A tradeoff of the design is a large nozzle-to-nozzle distance (1,27mm) and a rather small maximal printing frequency (< ~5kHz). The viscosity range is specified up to

250mPas but formation of proper drops from highly viscous fluids is not yet clear. Quantica printheads are in a ß-testing stage. For multi-material applications the price per print engine and the productivity play important roles. Quantica offers a good compromise here, although the printhead cannot process a range of fluids as large as the technologies men-tioned above.

2. Materials and methods: The rheology of UV dental materials

We regard UV dental materials for vat polymerization from two manufacturers (material A and B). The materials contain a high fraction of solids (ceramic fillers and pigments) with particle size < 1µm. To study the rheological properties and connect them to the chemical composition, the dental materials are compared to the UV base formulations without solids (material A0 and B0). The base formulations were provided by the manufacturers. The goal is to modify the rheological properties of the dental materials to obtain a proper drop formation in a Quantica printhead without compromising the material properties.

Polymers and sols (solid in liquid dispersions) are (to some degree) viscoelastic and shear-thinning. During drop-formation a high pressure (up to 1.5 hPa) and high shear rates ($\dot{\gamma} = 10^5$-$10^6\ 1/s$) act on the ink for a few 10µs. A shear-dependent viscosity does probably not reach an equilibrium state (as in a rheometer). Elasticity of polymers and sols strongly influences drop formation [Mackley, 2016]. In oscillatory and vibra-tional rheology, (linear) viscoelasticity is characterized by a storage module G′ and a loss module G″ which describe the spring-like behavior (G′), resp. the viscous dissipation (G″) of a viscoelastic fluid. The relation between shear stress $\sigma(t)$ and shear strain $\gamma(t)$ of a viscoelastic fluid is expressed as:

$$\sigma(t)=(G'+iG'')\gamma(t);\ \sigma(t)=\sigma_0 e^{i\omega t};\ \gamma(t)=\gamma_0 e^{i\omega t}$$

The power per volume transferred to and from the liquid by the harmonic excitation illustrates the meaning of storage module (G′) and loss module (G″):

$$\frac{P(t)}{V}=\mathrm{Re}(\sigma(t))\bullet \mathrm{Re}\,(\dot{\gamma}(t))=\gamma_0^2\omega\left(\underbrace{G''\sin^2(\omega t)}_{\text{Dissipation}}-\frac{1}{2}\underbrace{G'\sin(2\omega t)}_{\text{Oszillation}}\right)$$

G′ and G″ depend on angular speed ω and the viscoelastic model [Barnes, 1989; Larson, 1999; Mackley, 2016]. For low viscosity fluids the simplest model is the Maxwell model (Fig. 3). The relation between shear stress $\sigma(t)$ and shear strain $\gamma(t)$ (resp. shear rate $\dot{\gamma}(t)$) in the Maxwell model is:

$$\dot{\gamma}(t)=\frac{\dot{\sigma}(t)}{G}+\frac{\sigma(t)}{\eta}$$

With a harmonic excitation ($\sigma(t)=\sigma_0 e^{i\omega t}$; $\gamma(t)=\gamma_0 e^{i\omega t}$) one obtains:

$$G' = \frac{\omega^2 \tau \eta}{1+(\omega\tau)^2} \text{ and } G'' = \frac{\omega\eta}{1+(\omega\tau)^2}$$

η is a Newtonian viscosity (damping factor),

$\tau = \eta/G$ a relaxation time, and G a shear modulus.

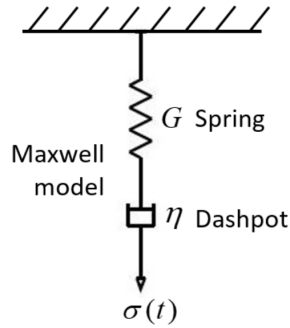

Figure 3: *The Maxwell viscoelastic model*

For real fluids (as the dental materials) more complex viscoelastic models are needed (*Fig. 9*). To capture the relevant rheological properties for drop formation G' and G'' need be extrapolated to frequencies for which the oscillation period corresponds to time scales for drop formation (10-100µs).

The shear-dependent viscosities of all materials were measured at 25°-80°C on an Anton Paar MCR302 rheometer with cone-plate measurement geometry (*Fig. 5*). At temperatures > 60°-70°C the viscosities and Ohnesorge numbers lie in the printable range of high-viscosity printheads (*Fig. 6*).

Because the dental materials are not designed for processing at elevated temperatures the integrity was tested as follows: The UV-polymers were stored at 70°C for 96h. A UV LED with 405nm peak wavelength (M405L3, Thorlabs GmbH) was integrated into the UV module (P-PTD-UV) of the rheometer (Anton Paar MCR302). G' and G'' were measured in oscillatory mode at a frequency of *1Hz* with plate-plate geometry. When the UV-LED was switched on G' and G'' quickly increased, indicating the onset of the crosslinking reaction (*Fig. 7*). An effect of degradation due to heating was not observed for any material.

The viscoelastic properties of the UV polymers were studied on a high frequency rheometer (Trijet TriPAV, *Fig. 4*). A thin ink film is vibrated up to 10kHz. The vibration causes a squeeze flow inside the sample from which G' and G'' can be extracted [Mackley, 2016]. The measured data allows to fit a viscoelastic model and to extrapolate G' and G'' to $f = 100kHz$ (*Fig. 10*). It should be mentioned that the TriPAV is an experimental measuring device, and we found it difficult to reproduce measuring results.

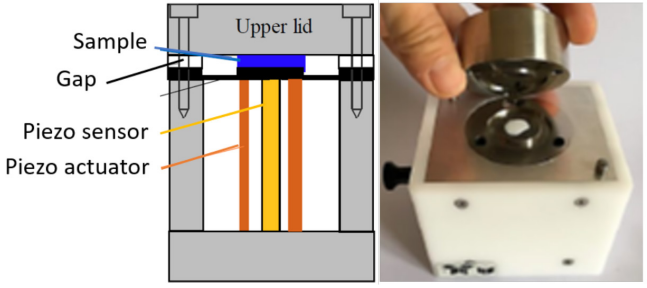

Figure 4: *The Trijet TriPAV vibrational rheometer (source: Trijet)*

3. Results and discussion

All measurement results were averaged over three measurement series. The shear rate sweep of all materials at 30°C and 70°C is shown in *Fig. 5*. The UV base formulations A0 and B0 show a nearly Newtonian behavior. It follows that the non-Newtonian behavior of materials A and B is caused by the solid load (sterically stabilized ceramic fillers and pigments). Material B is stronger shear-thinning than material A, reflecting the higher solid load of material B. The viscosity of material A depends stronger on temperature than viscosity of material B.

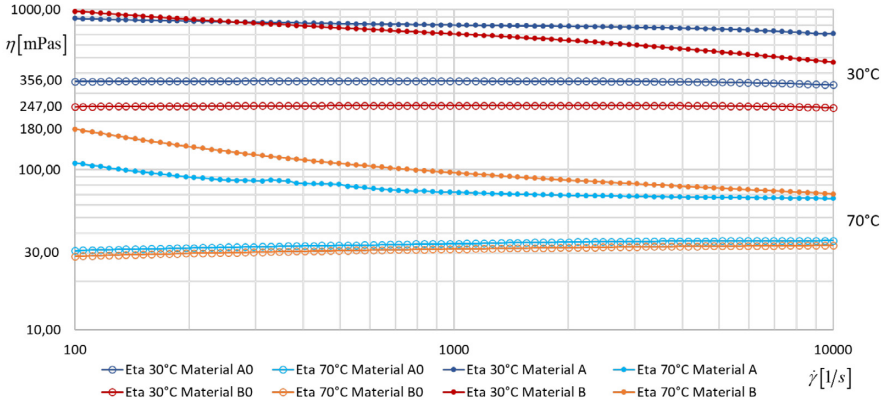

Figure 5: *Shear-dependent viscosities of materials A, A0, B, B0 at 30°C and 70°C*

In *Fig. 6* the Ohnesorge numbers of materials A and B are calculated at 70°C for the nozzle diameter of the Quantica printhead (60µm). We expect an extended range of printable fluids for high-viscosity printheads compared to standard piezo printheads.

	Material A	Material B
Temperature	70°C	70°C
Viscosity at 10000 1/s	~66 mPas	~70 mPas
Surface tension	~32 mN/m	~45 mN/m
Density	1,5 g/cm³	1,7 g/cm³
Nozzle diameter	60 µm	60 µm
Ohnesorge number	**~1,2–1,3**	**~1,0 –1,1**

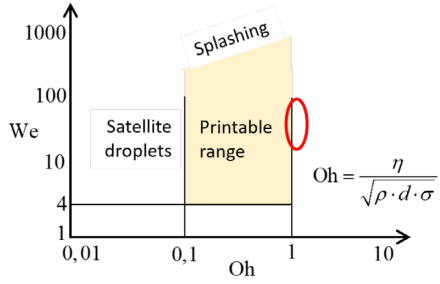

Figure 6: *Ohnesorge numbers of materials A and B at 70°C*

Curing tests of materials A and B are shown in *Fig. 7*. Storage module *G´* and loss module *G˝* quickly increase after the UV-LED is switched on. The UV-polymers were stored at 70°C for 96h and cured at 80°C. For comparison storage and curing was done at room temperature. The cross-linking reaction is accelerated at 80°C but the UV-polymers always fully cure and no degradation of the materials was observed.

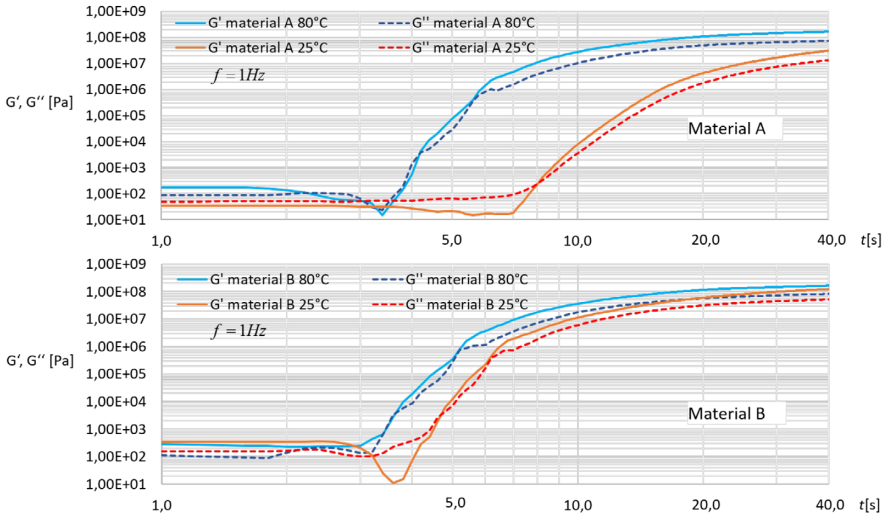

Figure 7: *Increase of storage module G' and loss module G'' during exposure of the dental materials. The UV-LED is switched on at t = 1s, the oscillation frequency is 1Hz.*

The viscoelastic properties of the dental materials and UV base formulations were evaluated with the TriPAV at 70°C (*Fig. 8*). The base formulations are nearly Newtonian (*Fig. 5*). For a Newtonian fluid, the shear module G in the Maxwell model is infinite and the relaxation time is $\tau = \eta / G = 0$. It follows: $G' = 0$ and $G'' = \omega\eta$.

The measured loss module of A0 is fairly linear and the measured storage module lies within the error margin of the TriPAV. In difference, materials A and B show large storage modules. However, we found it difficult to reproduce measuring results within small margins.

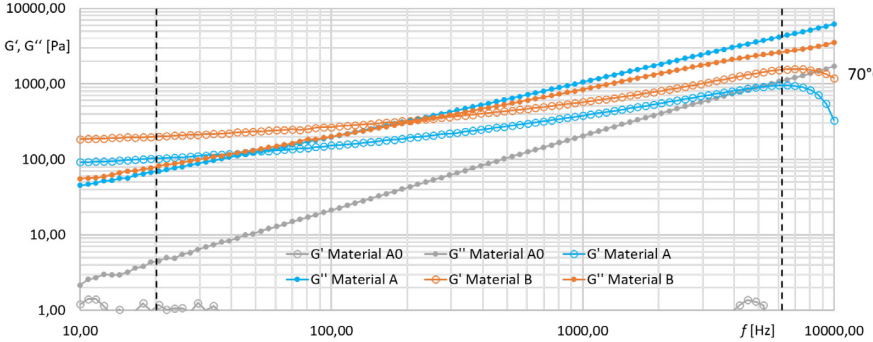

Figure 8: *Storage module G' and loss module G'' of the dental materials A and B and UV base formulation A0. Dashed lines indicate approximate range of validity of measurements.*

A viscoelastic model was fitted to G' and G'' of materials A and B. The complexity of the model should not be higher than needed. A plausible model that fits both data sets is the Maxwell-Wiechert model shown in Fig. 9. The relation between shear stress $\sigma(t)$ and shear strain $\gamma(t)$ (resp. shear rate $\dot{\gamma}(t)$) is

$$\dot{\gamma}(t)=\frac{\dot{\sigma}_j(t)}{G_j}+\frac{\dot{\sigma}_j(t)}{\eta_j} \text{ and } \sigma(t)=\sum_{j=1}^{4}\sigma_j(t)$$

A harmonic excitation ($\sigma(t)=\sigma_0 e^{i\omega t}$; $\gamma(t)=\gamma_0 e^{i\omega t}$) leads to:

$$G'=\sum_{j=1}^{3}\frac{\omega^2\tau_j\eta_j}{1+(\omega\tau_j)^2} \text{ and } G''=\sum_{j=1}^{3}\frac{\omega\eta_j}{1+(\omega\tau_j)^2}+\omega\eta_4$$

$$\eta^*=\frac{1}{\omega}\sqrt{G'^2+G''^2} \text{ (complex viscosity)}$$

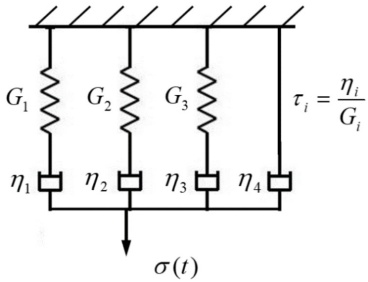

Figure 9: *The Maxwell-Wiechert viscoelastic model*

The complex viscosity η^* reflects the shear-thinning behavior of viscoelastic fluids. It is related but not proportional to the shear-dependent viscosity $\eta(\dot{\gamma})$. A fit of $G'(\omega)$, $G''(\omega)$ and $\eta^*(\omega)$, and extrapolations to a frequency of $f = 100kHz$ are shown in *Fig. 10*. The set of parameters is found in *Tab. 1*.

	Material A	Material B
τ_1	$2.80\cdot10^{-2}$s	$1.55\cdot10^{-2}$s
η_1	2.81 Pas	3.33 Pas
τ_2	$1.30\cdot10^{-3}$s	$6.1\cdot10^{-4}$s
η_2	0.180 Pas	0.171 Pas
τ_3	$8.0\cdot10^{-5}$s	$3.6\cdot10^{-5}$s
η_3	$6.2\cdot10^{-2}$Pas	$6.8\cdot10^{-2}$Pas
η_4	0.110 Pas	$5.1\cdot10^{-2}$Pas

Table 1: *Parameters in the Maxwell-Wiechert model (Fig. 10)*

The relaxation times τ_1, τ_2, τ_3 differ by 2-3 orders of magnitude. Relaxation times of polymers are $< \sim 1ms$ and can vary in a wide range. τ_2 and τ_3 could be relaxation times of the steric stabilization of solids as particles interact. A sheared flow distorts the microstructure of a sol as particles are forced to move relative to each other in planes. The restoring force to isotropy is Brownian motion what leads to much longer relaxation times. This would be τ_1.

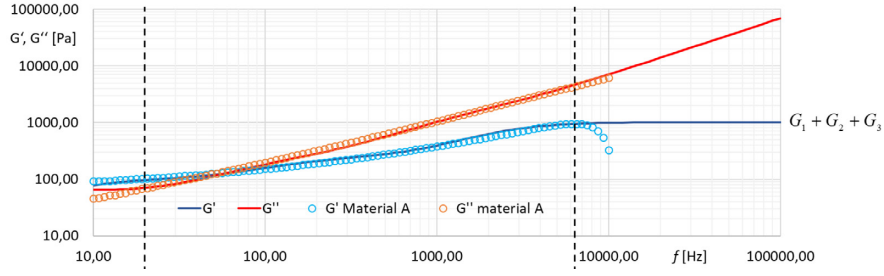

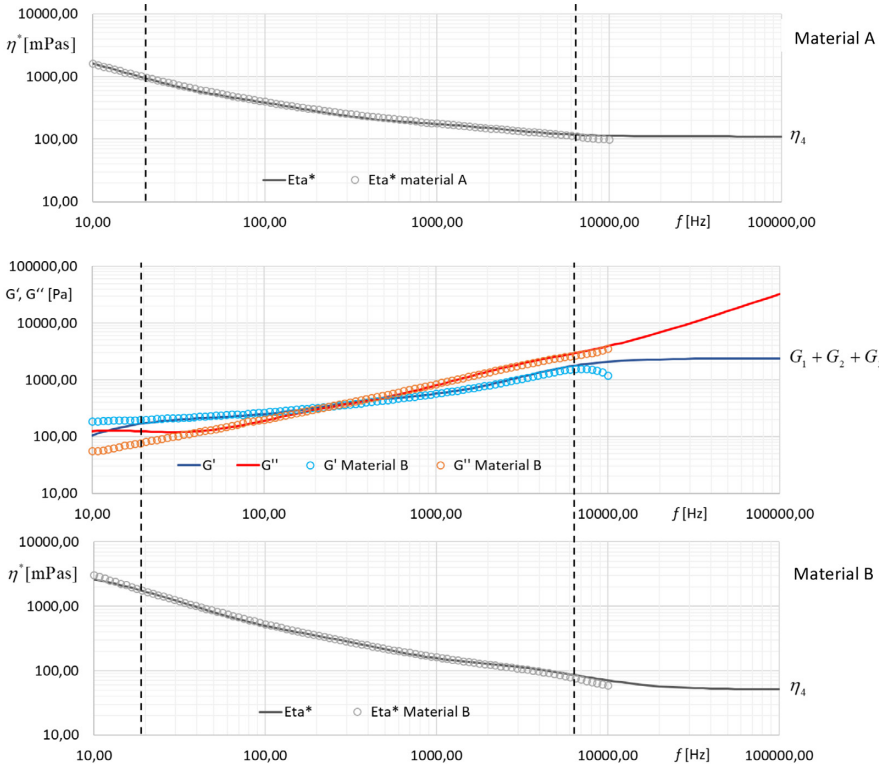

Figure 10: *Fits of the storage module G′, loss module G′′ and complex viscosity η^* of the dental materials A and B with aMaxwell-Wiechert model (Fig. 9). Dashed lines indicate approximate range of validity of measure ments.*

A first print test with dental material A was conducted by Quantica company at their site. It was shown that the UV-polymer can be printed with a Quantica printhead at 60°C. A strong formation of satellite droplets was observed. *Oh > 1 (Fig. 6)*. The connection of the rheology of non-Newtonian liquids to drop formation in the Quantica printhead is currently under progress.

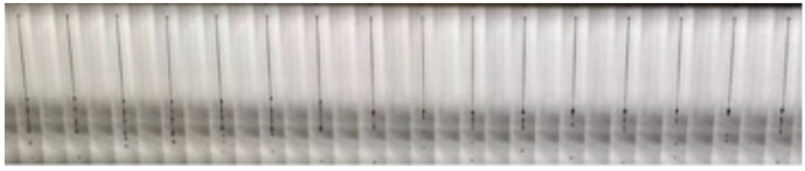

Figure 11: *Drop formation of dental material A in a Quantica printhead at 60°C. Printing frequency is 3,8kHz. Print test conducted by Quantica company.*

4. Acknowledgements

This project is conducted in cooperation with a manufacturer of UV-polymers for additive manufacturing of dental prosthesis. The authors thank Quantica company for their support and the conduction of a first print test.

5. References

Barnes, H.A., Hutton, J.F. and Walters, K., 1989. *An Introduction to Rheology*. Amsterdam: Elsevier.

Borrell, R., 2022. *Revolutionary piezo inkjet technology and printhead capable of jetting extreme viscosity inks* (presentation by Quantica company on the Industrial Print Integration 2022. Düsseldorf, Germany, 18−19, May 2022). Available at: https://www.youtube.com/watch?v=qsEd3FNPqlc.

Canon CrystalPoint, 2018. *OcéCrystal Point® technology*. Available at: <https://csa.canon.com/internet/wcm/connect/us/a3b369d5-60f3-46ff-a594-4048712207b7/oce-crystalpoint-technology.pdf?MOD=AJPERES&CVID=muEpOaD>.

Derby, B., 2010. Inkjet printing of functional and structural materials: fluid property requirements, feature stability, and resolution. *Annual Review of Materials Research*, 40(1), pp. 395−414. https://doi.org/10.1146/annurev-matsci-070909-104502.

Dimatix Galaxy 256 HM, 2015. *Galaxy PH 256/80 HM*. Available at: <https://www.fujifilm.com/us/en/business/inkjet-solutions/industrial-printheads/galaxy-ph-256-80-hm>.

Färber, L., Hartkopp, B., Quantica GmbH. 2021. *Material ejection system, print head, 3d printer, and method for material ejection*. European Patent Application EP 3 825 100 A1.

Galliker, P., 2024. *Electro-hydrodynamic printing and how to scale it towards economics* (presentation by Scrona company on the Advanced Inkjet Technology conference 2024. Fribourg, Switzerland, 29-31 January 2024).

International Organization for Standardization, 2021. *ISO/ASTM 52900:2021(en) Additive manufacturing−General principles − Fundamentals and vocabulary*. Geneva: ISO.

Jackson, N., 2019. *Expanding the boundaries of piezo inkjet* (presentation by Xaar company on The Inkjet Conference 2019, Düsseldorf). Available at:<https://www.youtube.com/watch?v=6WSSEX_8098>.

Larson, R.G., 1999. *The structure and rheology of complex fluids*. New York: Oxford University Press.

Mackley, M.R., Vadillo, D.C. and Tuladhar, T.R., 2016. Inkjet fluid characterization. In: S.D. Hoath, ed. *Fundamentals of inkjet printing*. Weinheim: Wiley-VCH.

Pekker, L., 2018. On Plateau-Rayleigh instability of a cylinder of viscous liquid. *Journal of Imaging Science and Technology*. 62(4): 040405. https://doi.org/10.2352/J.ImagingSci.Technol.2018.62.4.040405.

Serra, P. and Piqué, A., 2019. Laser-induced forward transfer: fundamentals and applications. *Advanced. Materials Technologies*, 4(1): 1800099. https://doi.org/10.1002/admt.201800099.

Wijshoff, H., 2008. *Structure and fluid-dynamics in piezo inkjet printheads*. PhD thesis, University of Twente.

Wijshoff, H., 2010. The dynamics of the piezo inkjet printhead operation. *Physics Reports*, 491(2-5), pp. 77−177. 10.1016/j.physrep.2010.03.003.

Xerox MDF, 2017. *Xerox® M Series industrial inkjet printheads*. Available at: <https://oem-printheads.business.xerox.com/products/m-series/>.